

## Optics on a Nanoscale Using Polaritonic and Plasmonic Materials

NSF NIRT Grant 0709323

PIs: **Andrey Chabanov**<sup>1</sup>, **Federico Capasso**<sup>2</sup>, **Vinothan Manoharan**<sup>2</sup>, **Michael Spencer**<sup>3</sup>,  
**Gennady Shvets**<sup>4</sup>, **Christian Zorman**<sup>5</sup>

<sup>1</sup>University of Texas-San Antonio, <sup>2</sup>Harvard University, <sup>3</sup>Cornell University,

<sup>4</sup>University of Texas-Austin, <sup>5</sup>Case Western Reserve University

The UT-Austin group has focused their research on an area of mid-infrared plasmonics. The practical rationale for this research direction is the importance of the mid-IR spectral range for biological and chemical sensing, infrared light harvesting for thermo-photovoltaics, and development of novel thermal emitters of tunable infrared radiation. We have used a single-crystalline polar semiconductor, SiC, for our experiments. Specifically, in collaboration with our colleagues at Sandia National Laboratory, we have fabricated and optically characterized SiC antennas which are set up on narrow Si pedestals over the wafer-thick Si substrate. Fabrication was performed using Reactive Ion Etching (RIE) of SiC at SNL. Pedestals were formed due to small over-exposure of SiC to RIE which resulted in undercutting the Si substrate. The resulting

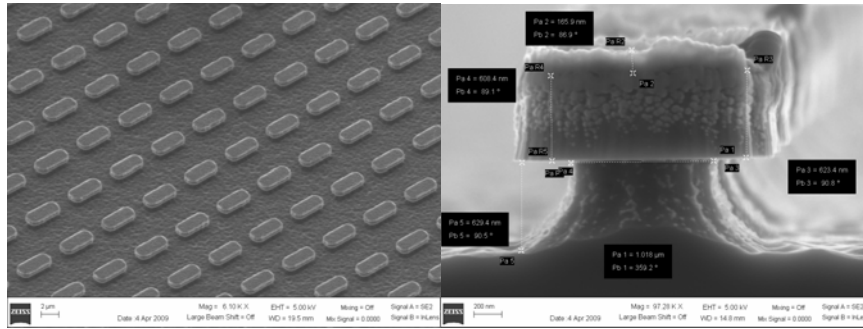


**Fig.1:** A square array of SiC antennas supported by Si pedestals over a Si substrate. Dimensions: antenna length  $L=3.8$  micron, antenna width  $W=1.6$  micron, SiC thickness:  $T=600$ nm, array periodicity:  $P=6$  microns. Left: individual antennas; Right: zoom-out showing a larger area of an array.

structure is shown in **Fig.1**. Optical spectra of the resulting antenna array were measured using an FTIR spectrometer with a microscope in reflectance mode. Polarized IR radiation was utilized to observe the dependence of the antenna polarizability on light polarization. Two light polarization: parallel (to the long dimension of the antenna) and perpendicular (to the same) were used. Experimental results were compared with the theoretical results from finite-elements frequency-domain numerical simulations using the COMSOL MultiPhysics package. The key result of this experiment was the observation of multiple antenna resonances of the SiC antennas. The spectra shown in **Fig.2** (solid lines: experiment, dashed lines: simulations) indicate that multiple antenna resonance can be excited. For example, the strongest peak at  $\omega = 810\text{cm}^{-1}$  correspond to the  $\lambda/2$  antenna resonance of the SiC antenna. This resonant is classified as a *plasmonic resonance* because it corresponds to  $\epsilon_{SiC} = -80 + 16i$ . A weaker resonance at  $\omega = 775\text{cm}^{-1}$  is classified as a dielectric antenna resonance because it corresponds to  $\epsilon_{SiC} = +92 + 10i$ . The resonance at  $\omega = 860\text{cm}^{-1}$  is classified as a  $3\lambda/2$  plasmonic resonance corresponding to  $\epsilon_{SiC} = -14 + 0.7i$ .

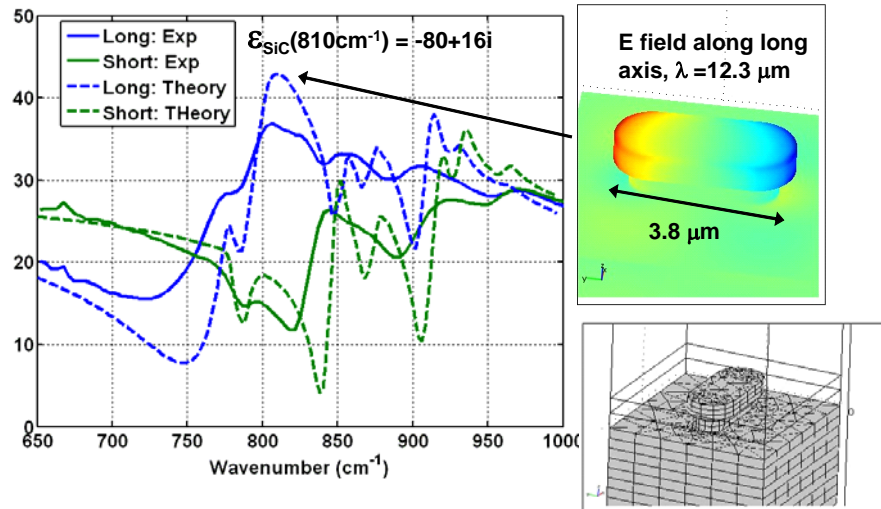


**Fig.2:** Reflection spectroscopy of SiC antennas shown in Fig.1. Experimental results are compared with and are in good agreement with the theoretical results from finite-elements frequency-domain numerical simulations. Multiple antenna resonances, both dielectric and plasmonic, can be excited over the broad frequency range. The insets, lower and upper, show cell for numerical simulations and the antenna surface charge distribution at a resonant wavelength  $\lambda=12.3 \mu\text{m}$ .

The Harvard group has focused their research on engineering liquid metamaterials, or *metafluids*, whose optical properties can be controlled by an external signal. Active control of optical and near-IR properties of water can be achieved by using a concept of Artificial Plasmonic Molecules (APMs) that are synthesized in emulsions and appropriately shaped to enable strong resonance response (**Fig.3**). Specifically, we have shown that nanoshell trimers can be used as a model system for magnetic resonance engineering. These new metamaterials will be used as an actively controlled component in applications such as IR imaging and liquid-liquid waveguides that guide light owing to the change in both electric permittivity and magnetic permeability.

The assembly of colloidal clusters starts with gold nanoshells as spherical building blocks. Nanoshells consist of silica cores surrounded by metallic shells, and their plasmon resonances can be tuned from the visible to near-infrared wavelengths by varying their core-shell aspect ratios. The nanoshells are next coated with a dielectric, which defines the gap separation in the nanoparticle clusters. Here, the polymer poly(ethylene) glycol yields  $\sim 2 \text{ nm}$  separations between nanoshells in the dried state (**Fig.3**). The polymer-coated nanoshells are then assembled into clusters by placing a droplet of the functionalized nanoshells onto a hydrophobic substrate and drying it slowly at room temperature. Capillary forces draw the nanoshells closer together until the droplet completely evaporates and the nanoshells cluster, held together by Van der Waals forces.

A single trimer has been probed by incident *s*- and *p*-polarization, which correspond to the electric field in, and normal to, the trimer plane, respectively. A gap separation of  $2.5 \text{ nm}$ , which is consistent with the TEM image, has been used in calculations to match the calculated and the experimental electric dipole peak position. A comparison between the experimental and theoretical spectra showed good agreement. The *s*-polarized spectra in both cases have an electric dipole peak near  $1200 \text{ nm}$  and higher order modes at  $600\text{-}700 \text{ nm}$  (**Fig.3**). Here, any

magnetic dipole peak is obscured by the stronger electric dipole mode. The *p*-polarized spectrum has a sharp peak near 700 nm, which represents out-of-plane plasmon resonances (**Fig.3**).

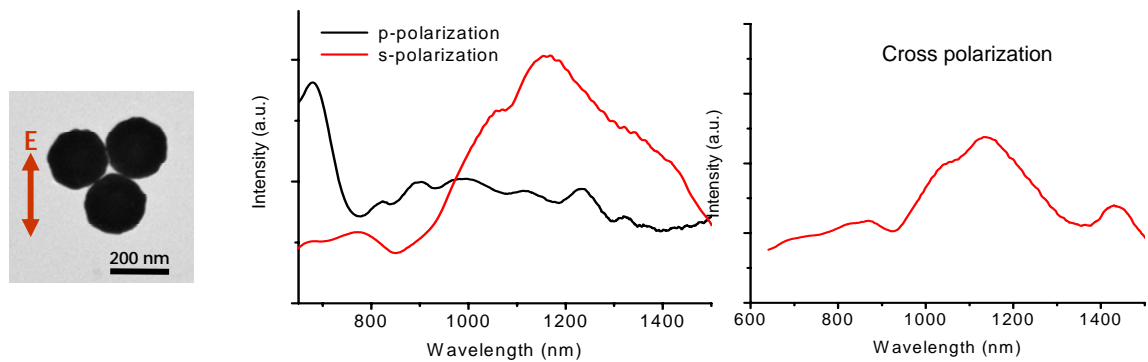


**Fig.3:** TEM image and scattering spectroscopy of a single nanoshell trimer.

When a crossed polarizer is placed in the light path, a narrow peak near 1400nm becomes visible (**Fig.3**). There is strong evidence that this feature is the magnetic dipole. Firstly, a direct calculation of the magnetic dipole shows a sharply peaked magnetic dipole near 1400nm. Secondly, the linewidths of the theoretical magnetic dipole and experimental feature are distinctly narrow and agree well with each other. Finally, the peak is significantly red-shifted relative to the electric dipole, which is consistent with electrostatic theory.